Reprinted from ENVIRONMENTAL SCIENCE & TECHNOLOGY, Vol. 24, 1990

Nitric Acid Concentrations in Southern California Museums

Lynn G. Salmon, William W. Nazaroff,† Mary P. Ligocki, Michael C. Jones, and Glen R. Cass*

Environmental Engineering Science Department and Environmental Quality Laboratory, California Institute of Technology, Pasadena, California 91125

■ Measurements were made during two seasons at five Los Angeles area museums to determine the concentrations of nitric acid in outdoor and indoor air. Mean seasonal indoor nitric acid concentrations ranged from <0.1 to 1.5 $\mu g/m^3$ corresponding to less than 1–40% of the outdoor nitric acid concentration, depending on building construction and ventilation system design. A mathematical model was applied to determine whether indoor/outdoor HNO_3 concentration ratios can be predicted from data on building parameters and ventilation system design. Good agreement between predicted and measured values was found. The rates of deposition of total inorganic nitrate onto vertical surfaces due to gas-phase plus aerosol-phase pollutants were measured and found to vary from 0.2 to 5.8 ng m^{-2} s^{-1}. Measurements indicate that nearly all of this deposition flux was delivered due to deposition of gas-phase species, but comparison to theoretical HNO_3 transport calculations suggests that gaseous species in addition to HNO_3 contribute to the observed accumulation of inorganic nitrate.

Introduction

A problem of increasing concern to those responsible for museum collections is the intrusion of air pollutants from the outdoor atmosphere. There is substantial evidence that air pollutants such as ozone, sulfur dioxide, nitrogen dioxide, and particulate matter cause significant damage to cultural property (*1*). A variety of nitrogenous air pollutants occur as a mixture in outdoor air, including nitrogen dioxide, nitric oxide, aerosol nitrates, nitrous acid, and nitric acid (*2*). However, little is known about nitric acid concentrations inside typical facilities where works of art are displayed.

Prolonged exposure to atmospheres containing oxides of nitrogen is known to cause deterioration of materials including dyes, textile fibers, plastics, rubber, and metals (*2*). For example, exposure studies have found fading and yellowing of a variety of textile dyes (*3–5*), degradation accompanied by loss of tensile strength of cotton and some man-made fibers (*6–7*), and surface corrosion of metals (*8–13*).

In several of these studies, the identity of the damaging agent has not been explicitly determined because of the coexistence of the various nitrogenous pollutants in the atmosphere. However, in a study of the NO_2-induced fading of natural and synthetic artists' colorants, nitric acid and other copollutants were specifically removed so that the effect of nitrogen dioxide alone on the pigments could be determined. NO_2 was found to cause only minor fading (*14*), so it is expected that a copollutant species, such as nitric acid, may have caused the damage attributed to the oxides of nitrogen in some past studies.

The deleterious effect of air pollution on cultural artifacts has been recognized in a general way for over a century. A study of the protection of the paintings in the National Gallery, London, from damage due to air pollution was published as early as 1850 (*15*). An extensive review of the concentration of air pollutants found in museums was presented by Thomson in 1965 (*16*). He advocated several important steps in the protection of museum collections including the use of building air filtration equipment to reduce air pollutant intrusion and the monitoring of indoor concentration levels as part of routine conservation efforts. A few studies of the ozone concentration in art galleries exist (*17–20*), and the relationship between indoor and outdoor levels of sulfur dioxide air pollution was measured by Hackney (*21*) in both air-conditioned and non-air-conditioned museums in London and Dublin. However, little research on the levels of other pollutants in museums has been performed, and essentially nothing is known about indoor HNO_3 concentrations.

Techniques for measuring the atmospheric concentration of nitric acid have been developed recently (*22–29*). A comprehensive survey of outdoor nitric acid levels in the Los Angeles Basin completed during 1986 (*24*) demonstrated that annual average atmospheric nitric acid levels range between 1.7 and 6.9 $\mu g/m^3$ (0.7–2.7 ppb) with maximum concentrations up to 21 $\mu g/m^3$ (8 ppb) during a 24-h sampling period as measured by the denuder difference method. Previous studies have shown that measured HNO_3 concentrations in the South Coast Air Basin surrounding Los Angeles have reached approximately 51 $\mu g/m^3$ (20 ppb) over short (2–6-h) time periods (*25, 26*).

The purpose of the present study is to determine the indoor and outdoor nitric acid concentrations at several museums in southern California. Measurements of the inorganic nitrate flux to the surfaces inside museums will be reported. The relationship between indoor and outdoor nitric acid levels then will be explored through indoor air quality modeling.

Measurement Plan

An air monitoring network was established at southern California museums to measure both indoor and outdoor gas-phase nitric acid concentrations, rates of gaseous and aerosol nitrate deposition onto building surfaces, and building characteristics such as the rate of air exchange with the outdoors. Sampling was conducted during two separate periods, one in the summer (July 2 through August 31, 1987) and one in the winter (November 23, 1987, through January 30, 1988) to account for seasonal variations in nitric acid levels.

Five museums were included in the study: the J. Paul Getty Museum, Malibu; the Norton Simon Museum, Pasadena; the Scott Gallery on the grounds of the Huntington Library, San Marino; the Southwest Museum, Los Angeles; and the Sepulveda House, on the grounds of El Pueblo de Los Angeles State Historic Park in downtown Los Angeles. These sites were chosen so that a variety of building types with different ventilation systems could be studied. The characteristics of each site are described in more detail in the next section, and a summary of the sites is presented in Table I.

Description of Museum Sites. The Sepulveda House is at one extreme with respect to indoor climate control. The two-story structure is a former private residence built in 1887 and converted for use as a museum. It has no system for regulating the indoor air temperature or hu-

†Present address: Department of Civil Engineering, University of California, Berkeley, CA 94720.

 0013-936X/90/0924-1004$02.50/0

Table I. Indoor/Outdoor Nitric Acid Measurement Sites

site	use[a]	HVAC type[b]	surface area, m^2	vol, m^3
Sepulveda House, Los Angeles	1	I	1710	1200
Southwest Museum, Los Angeles	2	II	830	840–940[c]
Norton Simon Museum, Pasadena	3	III	16800	21540
Virginia Steele Scott Gallery, San Marino	3	III	3060	2530[d]
J. Paul Getty Museum, Malibu	3	III	620	600[e]

[a] Use: (1) historical museum, (2) archeological museum, (3) art museum. [b] Heating, ventilation, and air-conditioning (HVAC) system type: (I) not air conditioned, large openings to the outdoors; (II) partial forced ventilation system (see text); (III) modern heating, ventilation, and air-conditioning plant with activated carbon filtration. [c] Volume and surface area are for the California Room only. Higher limit on building volume includes volume inside display cases. [d] Volume and surface area are for the occupied portion of the west wing only. [e] Volume and surface area are for gallery 121 only.

midity and relies on relatively large openings in the building shell for air exchange with the outdoors. When the building is open to the public, two doors on the lower floor are often kept open, causing large air-exchange rates. Even when the doors are closed, large gaps around doors and windows permit considerable air flow through the building.

The Southwest Museum is a multistory poured concrete building built in the early 1900s. The main portion of the building has no air cooling, but a system of high-powered fans circulates air through this section of the building. The California Room, in which the deposition plates and other sampling equipment were located, has a local forced-air heating and cooling system, which draws air from a hallway that connects the California Room to the unconditioned main portion of the building. This room is largely isolated from the main portion of the building, and the air-exchange rate in this room is lower than in the building as a whole.

The Norton Simon Museum, the Scott Gallery, and the Getty Museum are each modern buildings with sophisticated air-conditioning systems that include both particle filtration and an activated carbon bed for gaseous pollutant removal. At the Norton Simon Museum, the make-up air from outdoors passes through a fibrous mat filter and then through an activated carbon filter, before being blended with return air that has passed through a fibrous mat filter. The air is then conditioned for proper temperature and humidity and distributed to the building through a network of porous ceiling tiles. The supply-air blower has been shut off to improve temperature control; therefore, the flow rate of outdoor make-up air is lower than the original design value. The building is well sealed and only open to the public for 6 h/day, 4 days/week. The deposition plates and sampling equipment were located in gallery 8, far removed from the entrance doorway.

At the Scott Gallery, the building was originally operated with 25% outdoor make-up air, which would be blended with the return air, passed through a fibrous filter, conditioned, and then distributed to the building (*20*). During the course of the present study, an activated carbon filter was added to this ventilation system to remove ozone, and the flow rate of outdoor make-up air was effectively reduced to zero by closing the intake dampers for the purpose of improving thermal control. With the modified mechanical ventilation system, air exchange between the indoors and outdoors results entirely from infiltration through cracks in the building shell and through door oepnings. Air samplers were located in a foyer at the end of the gallery farthest from the main entrance to the building. During normal operation the main entrance doors were left open when the gallery was open (1:00 p.m. to 4:30 p.m. daily). During the winter sampling period, a second set of exterior doors near our sampling equipment was often opened briefly to allow access to construction in the adjacent Brown Room Gallery, which may have allowed slightly higher than usual pollutant infiltration from outdoors.

The Getty Museum is located near the ocean and northwest of downtown Los Angeles. This area is generally considered to be upwind of major air pollution sources, and outdoor pollution levels at this site were lower than at any of the other sites. At the Getty Museum, air supplied by the mechanical ventilation system passes through bag filters for particle removal and through a charcoal filtration bank for ozone control. According to architectural specifications, the outdoor air supply rate is 10–20% of the flow rate through the system, with the remainder recirculated from the conditioned space. The mechanical ventilation system that serves the galleries on the main (antiquities) floor, where the measurements reported in this paper were made, is only operated between 8:00 a.m. and 6:00 p.m. Furthermore, during business hours, 10:00 a.m. to 5:00 p.m. daily (excluding Mondays), gallery doors opening onto a courtyard are generally left open, allowing untreated outdoor air to enter the galleries, despite the attempt to pressurize the building so that the airflow through these doors is outward.

Ambient Air Sampling. The objective of the experimental program is to measure long-term average HNO_3 concentrations that can be compared to an air quality model for long-term average concentrations. The availability of short-term average or continuous HNO_3 concentration data would permit the more sophisticated short-term average indoor air quality model of Nazaroff and Cass (*20*) to be tested for its ability to track indoor HNO_3 concentrations over time, but at much greater expense. From the point of view of assessing the potential for materials damage effects over long periods of time, measurement and modeling of long-term average HNO_3 concentration exposures should be sufficient. Therefore, a network of manual intermittent nitric acid sampling systems similar to those used in previous outdoor nitric acid measurement programs (*24*, *25*) was installed in a gallery at each museum, and a duplicate set of equipment was placed outdoors on the grounds of each site. Sampling each season took place during 24-h periods, once every 6 days. Filter samples were loaded at all sites one day in advance and equipment timers were set so that simultaneous sampling was performed at all sites.

The sampling system included two subsystems for obtaining gas-phase nitric acid measurements, one by the denuder difference method (*24–26*, 28, *29*) and the other via the tandem filter method (*22*, *24–26*, *29*). With the denuder difference method, measurement of nitric acid was made by first passing air at a rate of 28.3 L/min through a Teflon-coated cyclone separator [for coarse particle removal (*30*)]. The system then branched into two parallel sampling lines each controlled by a critical flow orifice to maintain the air flow rate in each sample line at 4.9 L/min, with the remaining air flow of 18.5 L/min used for a separate aerosol measurement experiment that is not discussed here (*31*). Air traveling in the first branch of the HNO_3 measurement system traversed a magnesium oxide

coated diffusion denuder, which removed nitric acid but allowed the fine aerosol nitrate to pass to a nylon filter (Gelman Nylasorb, 47-mm diameter, 1-μm pore size) where it was collected. A parallel nylon filter collected total inorganic nitrate (i.e., nitric acid plus fine aerosol nitrate) that did not pass through the diffusion denuder. Nitric acid levels were determined by taking the difference between fine aerosol nitrate and total inorganic nitrate levels.

The tandem filter method provided an additional measurement of nitric acid that was available in the event that a denuder difference method sample should fail to be collected. In the tandem filter method, air flowed at a rate of 3 L/min through an open-face, 47 mm diameter Nuclepore filter holder that contained two filters in series. Nitric acid was collected on a nylon backup filter (Gelman Nylasorb, 1-μm pore size) after any particles (including aerosol nitrate) were removed by an open-face inert poly(tetrafluoroethylene) (PTFE) prefilter (Gelman Teflo, 2-μm pore size). Studies detailing the merits of each method are available in the literature (*22*, *25*, *26*, *29*, *32*).

After sample collection, filters were immediately transferred to sealed Petri dishes and refrigerated until analysis to avoid loss of volatile material. To analyze, water-soluble material was extracted from the filters by placing them in 10 mL of dilute $Na_2CO_3/NaHCO_3$ (eluent for the ion chromatograph) and mechanically shaking them in sealed containers in a refrigerated room for 3 h. All samples were analyzed for nitrate ion by ion chromatography using a Dionex Model 2020i ion chromatograph. The analytical precision of 0.072 $\mu g/m^3$ was determined from replicate analysis of 77 filter samples. Analytical precision is equal to instrument precision (0.49 μg/filter)/average volume of air sampled per filter (6.8 m^3). Laboratory and field blank samples also were analyzed to determine background nitrate levels.

Wall Deposition Plates. A set of two wall deposition plates was employed at each site to determine the rate of gas-phase and aerosol-phase nitrate deposition onto museum surfaces. Deposition plates consisted of membrane filter material mounted in flat (3 mm thick) aluminum frames attached to building walls so that air will flow over but not through the deposition plate surfaces. The edges of the frames were beveled to minimize disruption of the boundary layer airflow along the wall. Because nitric acid is known to sorb onto aluminum, Teflon-coated deposition plate frames were used for total inorganic nitrate collection.

Nylon filter material of the same type as used in the air sampling program was used as a collection surface for total inorganic nitrate (nitric acid plus aerosol nitrate) because this material is known to bind and retain both HNO_3 and aerosol nitrate (*33*). To determine the nitric acid flux to surfaces, it was necessary to subtract an estimate of the deposited particulate nitrate from the total inorganic nitrate collected on the nylon deposition surfaces. Deposition plates covered with large sheets (20 × 25 cm) of Teflon membrane filter material (Gelman Zefluor, 1-μm pore size) were employed as deposition substrates for aerosol nitrate. Being chemically inert, the Teflon substrates collected particulate nitrate material, but not nitric acid (*33*).

The deposition plates were placed on museum walls prior to each seasonal sampling period, with a separate set of plates used for the winter and for the summer studies. With the exception of Sepulveda House, deposition plates were located in galleries where works of art were displayed at each site. The plates were placed at heights of 2.5–4.0 m in locations that would avoid interference from the public. The deposition surfaces were exposed for 10–12 weeks during each sampling period and then removed and analyzed by ion chromatography for the inorganic nitrate collected.

Air-Exchange Rate Measurements. Building air-exchange rates were measured by two tracer gas techniques. During each of the summer and winter sampling periods, a perfluorocarbon tracer (PFT) system (*34*, *35*) was employed at each of the five museum sites to determine the long-term average building air-exchange rate during each period. In supplemental field work during the spring of 1988, a tracer-gas decay technique with sulfur hexafluoride as the tracer gas (*36*) was used at three of the museum sites (Sepulveda House, Norton Simon Museum, and Scott Gallery) to determine the air-exchange rate over a period of a few hours to a few days (ref 37, Chapter 6).

Nitric Acid Removal by Ventilation System Filters. The nitric acid removal due to the ventilation system filters that are used within museums to protect against ozone and particle intrusion from outdoors was tested at the Norton Simon Museum. The ambient nitric acid sampling equipment described earlier was placed in the ventilation system for a 24-h period on September 24, 1987. One set of sampling equipment was placed in the chamber where outdoor make-up air is introduced into the building. A second set was placed downstream of both a fibrous mat particle filter and an activated carbon bed. The nitric acid removal efficiency of the set of ventilation filters was then determined by comparing the upstream and downstream nitric acid concentrations. Further testing of the ventilation system at the Norton Simon was performed on May 1, 1989, to measure nitric acid losses in the ducts and in the porous ceiling tiles through which the air traverses before entering the gallery. Four sets of sampling equipment were deployed: one at the entrance to the ventilation ducts, one at the exit from the ventilation ducts above gallery 8 before the ceiling tiles, one in gallery 8 under the ceiling tiles, and the fourth in the location where seasonal nitric acid measurements were made.

Results

Nitric Acid Concentrations. The five museums included a wide range of building ventilation system types. As might be expected, higher indoor nitric acid levels were found in the Sepulveda House, which combines a high air-exchange rate with a lack of climate control equipment. The more tightly controlled facilities with custom-engineered heating, ventilation, air-conditioning (HVAC), and pollutant removal systems had low indoor nitric acid concentrations. In the latter case, the low concentrations are due to a combination of pollutant removal as air passes through the HVAC system plus longer retention times for air inside these buildings, which permits concentrations to decline as HNO_3 reacts with indoor surfaces (including the collections).

Table II summarizes the mean summer and winter nitric acid concentrations, including the highest measured concentration at each site determined by the denuder difference method. Past studies have shown that the tandem filter method (*25*, *26*) suffers from a positive HNO_3 artifact, and this was evident in the data collected during this study. Therefore, only the results from denuder difference measurements are reported.

Figure 1 more clearly illustrates the relative differences between the sites on average, while Figure 2 displays the daily variation in nitric acid concentration, both indoors and outdoors, at all museum sites. As can be seen in Figure 2, nitric acid levels inside Sepulveda House are the highest, typically 40% of the HNO_3 concentration outdoors. The indoor nitric acid concentration in the California Room

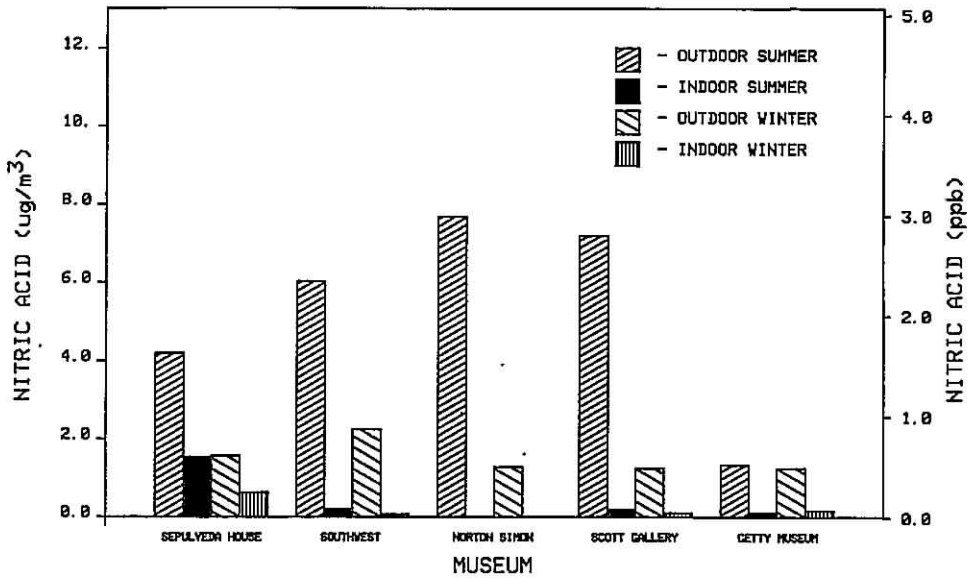

Figure 1. Mean indoor and outdoor nitric acid concentrations measured by the denuder difference method, summer 1987 and winter 1987–1988.

Table II. Indoor/Outdoor Nitric Acid Concentrations ($\mu g/m^3$)[a] Measured by the Denuder Difference Method

		average[b]		max 24-h	
site	season	outdoor	indoor	outdoor	indoor
Sepulveda House	summer	4.20 ± 0.68	1.53 ± 0.18	8.81	2.43
	winter	1.57 ± 0.27	0.63 ± 0.14	3.01	1.37
Southwest	summer	6.03 ± 0.83	0.21 ± 0.05	12.71	0.43
	winter	2.24 ± 0.48	0.07 ± 0.04	5.17	0.16
Norton Simon	summer	7.68 ± 0.88	<0.10	13.01	<0.10
	winter	1.28 ± 0.31	<0.10	3.43	<0.10
Scott Gallery	summer	7.19 ± 0.72	0.20 ± 0.05	10.52	0.56
	winter	1.24 ± 0.27	0.10 ± 0.04	3.76	0.29
Getty Museum	summer	1.33 ± 0.27	0.11 ± 0.04	3.12	0.25
	winter	1.24 ± 0.24	0.17 ± 0.04	2.85	0.36

[a] 1 ppb = 2.58 $\mu g/m^3$. [b] Mean ±1σ uncertainty of the mean.

of the Southwest Museum, on the other hand, remains at a fairly constant low level during each season despite outdoor fluctuations. The typical indoor/outdoor HNO_3 ratio at the Southwest Museum was approximately 4–5%.

Among the five sites, the Norton Simon Museum had the lowest indoor nitric acid levels, despite having the highest outdoor HNO_3 concentration. Indoor HNO_3 levels at the Norton Simon were barely detectable and generally less than 1–2% of the outdoor HNO_3 concentration. The Scott Gallery also had low indoor HNO_3 levels, which averaged 3–11% of the outdoor concentration. However, nitric acid concentrations at the Getty Museum were approximately 11–18% of those outside, which is noticeably higher than the indoor/outdoor HNO_3 concentration ratios seen at other museums that have pollutant removal systems. Indoor concentrations of air pollutants are higher than would be the case if the courtyard doors were kept closed.

Deposition to Surfaces. One mechanism for nitric acid removal from the air in museums is through deposition onto indoor surfaces, including items in the collection. Table III shows the *apparent* flux of inorganic nitrate from the gas phase to vertical surfaces at each site. These values are based on the total inorganic nitrate deposited on the nylon collection surfaces minus the particulate nitrate collected on the Teflon surfaces.

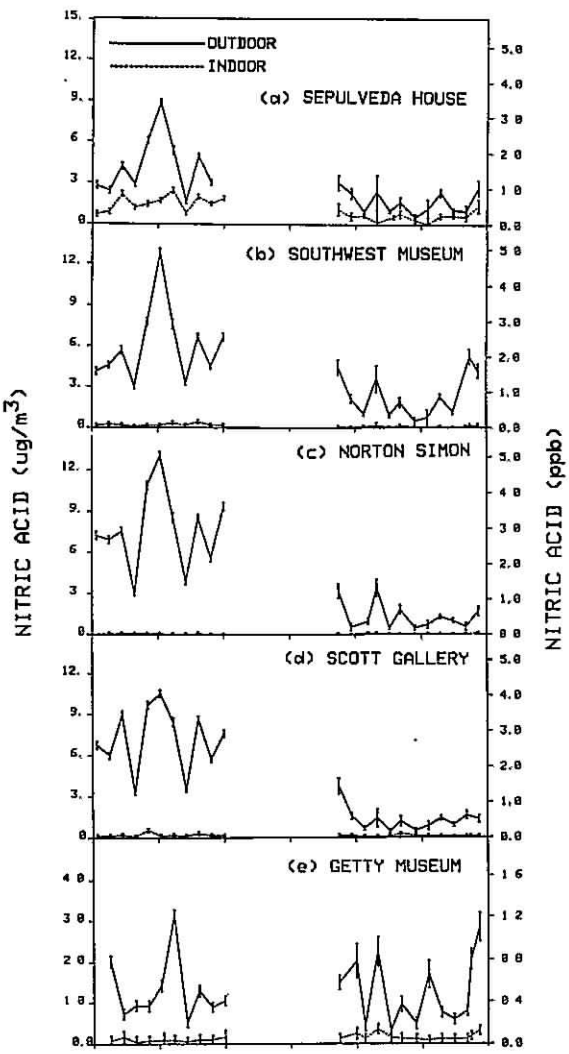

Figure 2. Daily variation in nitric acid concentration: a, Sepulveda House; b, Southwest Museum; c, Norton Simon Museum; d, Scott Gallery, e, Getty Museum.

Deposition velocities for transport of HNO_3 vapor to the walls at each museum site are presented in Table IV. "Measured" values were determined by dividing the apparent deposition flux of inorganic nitrate due to gaseous species by the mean indoor ambient HNO_3 concentration

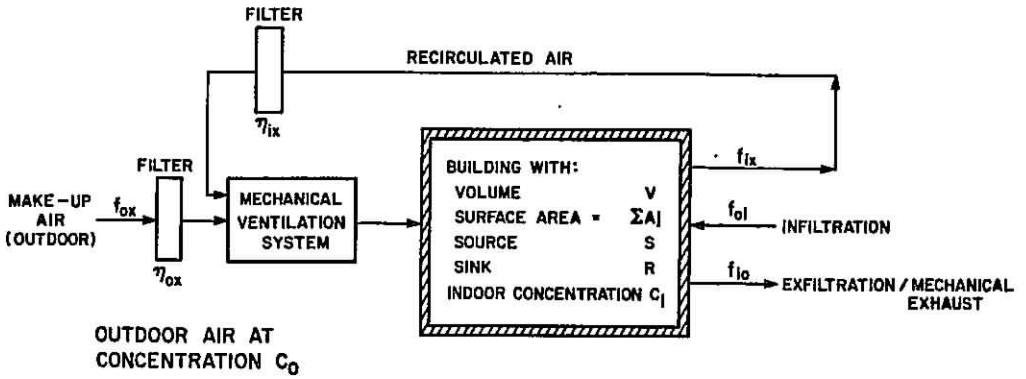

Figure 3. Schematic of a typical building ventilation system.

Table III. Measured Inorganic Nitrate Deposition to Vertical Surfaces

site	season	flux, ng m^{-2} s^{-1}: total inorg nitrate[a]	partic-phase nitrate[b]	apprnt gas-phase inorg nitrate[c]
Sepulveda House	summer	5.85 ± 0.21[d]	0.029	5.82 ± 0.21[d]
	winter	2.01 ± 0.11	0.031	1.98 ± 0.11
Southwest Museum	summer	1.76 ± 0.11	<0.006	1.76 ± 0.11
	winter	0.91 ± 0.08	<0.007	0.90 ± 0.08
Norton Simon	summer	0.18 ± 0.07	<0.006	0.18 ± 0.07
	winter	0.23 ± 0.07	<0.006	0.23 ± 0.07
Scott Gallery	summer	2.19 ± 0.12	0.0073	2.18 ± 0.12
	winter	0.63 ± 0.08	<0.006	0.63 ± 0.08
Getty Museum	summer	2.58 ± 0.13	<0.006	2.58 ± 0.13
	winter	2.21 ± 0.12	0.0096	2.20 ± 0.12

[a] Total inorganic nitrate accumulation onto a vertical nylon surface, which is thought to be a perfect sink for both gaseous HNO_3 and aerosol nitrate. [b] Particulate-phase nitrate accumulation onto a vertical Teflon surface, which is thought not to collect HNO_3. [c] Apparent gas-phase inorganic nitrate deposition to vertical surfaces based on the difference between collections on nylon and Teflon surfaces. [d] Error bounds expressed as $\pm 1\sigma$.

Table IV. Apparent HNO_3 Deposition Velocities to Vertical Surfaces (cm/s)

site	measured[a]: summer	measured[a]: winter	predicted[b]
Sepulveda House	0.38 ± 0.05	0.32 ± 0.07	0.09[c]–0.18[d]
Southwest Museum	0.85 ± 0.20	1.34 ± 0.75	0.07
Norton Simon	>0.18	>0.24	0.04
Scott Gallery	1.11 ± 0.31	0.62 ± 0.23	0.18
Getty Museum	2.37 ± 0.90	1.32 ± 0.31	0.29

[a] Ratio of apparent inorganic nitrate deposition from the gas phase (Table III) to long-term average indoor ambient HNO_3 concentration measured by the denuder difference method (Table II). Errors (1σ) propagated from division of these values. [b] Best estimate deposition velocity of gas-phase nitric acid based on near-wall airflow measurements at each site using methods presented in Chapter 7 of ref 37. [c] Case assumes natural convection-driven flow adjacent to walls when building is closed and turbulent flow in the core of the room when the building is open to the public. [d] Case assumes turbulent flow in the core of the room all the time.

at each site. Predicted deposition velocities were determined by calculation of the diffusion-limited flux of HNO_3 through the boundary layer adjacent to the walls in each building. These fluid–mechanical transport calculations were based on data from long-term measurements of surface–air temperature differences, short-term measurements of near-wall air velocities, and idealized representations of the complex air flow fields prevailing at each museum location. A detailed description of the basis for these predictions is provided elsewhere (*37*).

Air-Exchange Rates. A schematic representation of a building ventilation system is given in Figure 3. Airflows through the building ventilation system consist of outdoor make-up air plus air recirculated from the inside of the building back through the heating and cooling system. The results of outdoor air-exchange rate measurements made by both perfluorocarbon (PFT) and sulfur hexafluoride tracer techniques are presented in Table V. Data on the number of air changes per hour due to internal air recir-

Table V. Air-Exchange Rate Measurements (h^{-1})

site	outdoor air–exchange rate: PFT[a] summer 1987	PFT[a] winter 1987–1988	SF_6[b] spring 1988	internal air recirculn rate
Sepulveda House	2.1	1.6	3.6	0[c]
Southwest Museum (California Room)	0.3	0.3	*d*	*e*
Norton Simon	0.7	0.7	0.4	5.4[f]
Scott Gallery (West Wing)	1.0	3.4	0.3	8.2[f]
Getty Museum (gallery 121)	1.3	1.2	*d*	7.1[g]

[a] Long-term average building air-exchange rate determined by a perfluorocarbon tracer (PFT) over the season (*34*, *35*). [b] Air-exchange rate determined by sulfur hexafluoride tracer-gas decay over intervals of a few hours (Norton Simon) to 24 h (Scott Gallery and Sepulveda House) (*37*). [c] No internal recirculation system present. [d] Not measured. [e] Not determined, as there is no deliberate gaseous pollutant removal applied to the recirculated air. [f] Measured with a hot wire anemometer. [g] Estimated on the basis of architectural specifications assuming 15% outdoor make-up air.

culation through the building ventilation systems obtained from hot wire anemometry measurements and architectural specifications also are given in Table V. For the Getty Museum and the Southwest Museum, the rooms in which nitric acid concentrations were measured were treated as isolated chambers in computing the air-exchange rate. At the Scott Gallery, only the occupied portion of the west wing was considered as a single chamber for calculations, whereas, at the remaining two sites, the entire building was treated as a single chamber.

Except at the Scott Gallery, the PFT measurements show that ventilation rates at most sites did not vary greatly by season of the year. The wintertime ventilation rate at the Scott Gallery, measured by the PFT method, is unreasonably high and is not consistent with the operation of the building and its ventilation system. In the air quality modeling study discussed in a subsequent section of this paper, the outdoor air-exchange rate at the Scott Gallery will be based on the summer and spring experiments, which are in the range of 0.3–1.0 h^{-1}.

Nitric Acid Removal by Ventilation System Components. At the Norton Simon Museum, the concentration of HNO_3 in the chamber before the filter bank was 1.66 $\mu g/m^3$ (0.64 ppb). After the air was passed through the particle filter and activated carbon filter bed, the HNO_3 concentration was found to be 0.85 $\mu g/m^3$ (0.33 ppb), indicating a single-pass HNO_3 pollutant removal efficiency of 49% due to the particle filter plus activated carbon filter. Examination of HNO_3 losses, measured by the denuder difference method, as the ventilation air passes through the ducts and ceiling tiles at the Norton Simon Museum produced inconclusive results. The HNO_3 levels were so low that when measured by difference between the two filter substrates, the error bounds on the measured values were larger than the HNO_3 losses to the ducts and ceiling tiles. Nitric acid measurements made by the tandem filter method, however, suggest an HNO_3 loss of approximately 40% in one pass through the ducts and ceiling tiles between the fan room and the room in gallery 8.

Discussion

Deposition to Surfaces. The measured HNO_3 deposition velocities are larger than the theoretical predictions by factors ranging from 2 to 12 (Table IV). In addition, the measured fluxes at the Sepulveda House, at the Southwest Museum, and at the Getty Museum exceed the amount of HNO_3 entering the building with the ventilation air, as will be shown in a later section of this paper. Several possible explanations exist for the higher measured values:

1. Very low ambient HNO_3 concentrations were measured inside some museums. In particular, the Norton Simon and Southwest Museums had indoor concentrations that were just barely detectable, leading to large relative uncertainty in the mean and, thus, uncertainty in the measured deposition velocities. These two sites display the poorest agreement between measured and predicted deposition velocities. Modeling studies presented later in this paper show that the indoor concentration measurements and the deposition flux measurements at the Norton Simon Museum are, in an absolute sense, both consistent with the air fluxes and HNO_3 concentrations entering that building.

2. Deposition flux measurements were taken under conditions requiring many weeks for sample collection, and only one sample was obtained at each location. It is possible that losses of aerosol nitrate from the Teflon collection surfaces occurred (e.g., by decomposition of NH_4NO_3 over time). This would result in overpredicting the HNO_3 deposition flux, which is determined by difference between collection on the nylon and Teflon surfaces. However, application of theoretical deposition velocities (*38*) to the measured indoor particulate nitrate concentrations (*31*) indicates that the measured aerosol nitrate fluxes are reasonable.

3. Gaseous nitrogenous species in addition to nitric acid may be collected as nitrate on the nylon deposition surface. For example, it has been shown that nylon filters exhibit substantial affinity for HNO_2, and oxidation of NO_2^- to NO_3^- occurs in the presence of O_3. For long exposure times this conversion approaches 100%, creating a positive bias in HNO_3 determination on nylon substrates (*39*).

4. There is also evidence that NO_2 may be reduced to NO (*40*) and/or HNO_2 (*20, 41*) on indoor surfaces. Since NO_2 concentrations are generally much larger than HNO_3 concentrations, particularly in indoor air, the conversion to HNO_2 of a small fraction of the nitrogen dioxide molecules that strike the nylon surface, combined with the ability of the nylon surface to retain HNO_2, could, in combination with oxidation by ozone, imply a large increase in the nitrate deposition rate due to gas-phase species over that due to nitric acid alone.

5. The predicted deposition velocities are uncertain due to the need to extrapolate from typically 1 day of air flow measurements to conditions occurring over two seasons of the year.

The finding that the total inorganic nitrate accumulation on surfaces can exceed the flux due to HNO_3 plus aerosol nitrates in the room air holds possibly important implications for pollution control practices in museums. It may be necessary to remove other nitrogenous species in addition to HNO_3 and aerosol nitrates in order to assure that inorganic nitrate accumulation on surfaces is prevented.

Mathematical Modeling. Having gathered data on the ventilation system design in the various museums, it is possible to predict the indoor/outdoor ratio of nitric acid based on an air quality modeling procedure developed previously (*42*). The predicted values then can be compared to the actual measured indoor/outdoor ratios shown in Figure 4.

Assume that the building is represented as a single well-mixed chamber shown schematically in Figure 3. Writing a mass balance for nitric acid yields

$$V\frac{dC_i}{dt} = C_o f_{oi} + C_o(1-\eta_{ox})f_{ox} + C_i(1-\eta_{ix})f_{ix} - C_i\sum_j A_j v_{d_j} - C_i(f_{oi}+f_{ox}+f_{ix}) \quad (1)$$

where C_i and C_o are the indoor and outdoor nitric acid concentrations, respectively; f_{oi}, f_{ox}, and f_{ix} are the rates of air flow associated with infiltration, mechanical supply, and recirculation, respectively; η_{ox} and η_{ix} are the HNO_3 removal efficiencies for filters in the outdoor make-up air supply and air recirculation lines, respectively; A_j is the surface area of the jth interior surface; v_{d_j} is the pollutant deposition velocity onto the jth surfacece; V is the volume of the chamber; and t is time. Note that the summation of $f_{oi} + f_{ox}$ appearing in the last term of eq 1 is used to represent the exfiltration plus exhaust flow from the building, f_{io}: air can be considered incompressible for present purposes, and so the total flow rate into a building must equal the total flow rate out.

In eq 1 the generation and removal of nitric acid due to chemical reaction and gas-to-particle conversion processes is not considered. Previous work (*20*) showed that for two moderately polluted days, the net rate of indoor production of nitric acid by homogeneous chemical reaction could account for 13% of the indoor nitric acid. That study was

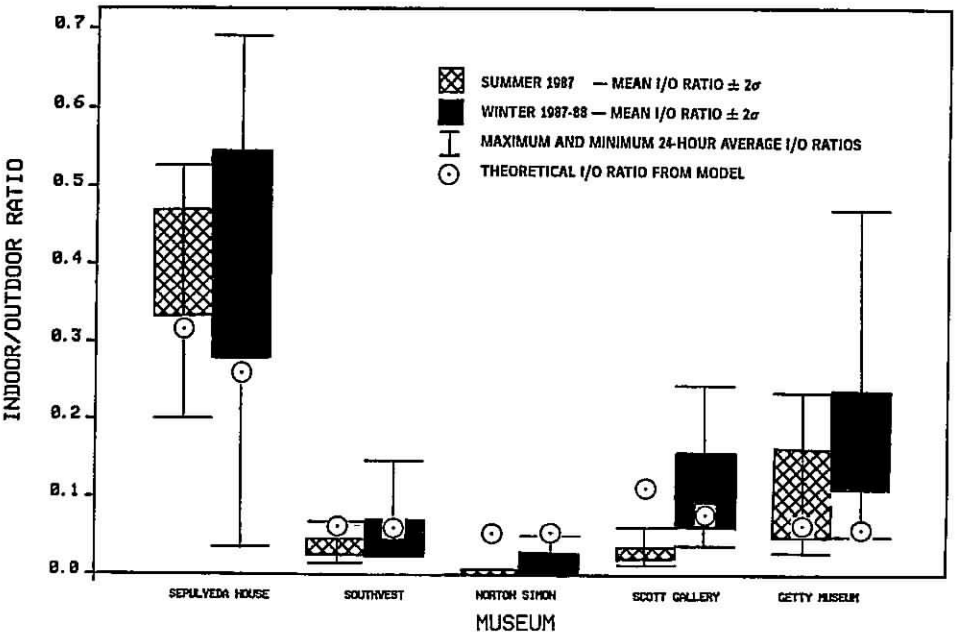

Figure 4. Indoor/outdoor nitric acid concentration ratios. The thin bars indicate the range of ratios measured over single 24-h periods at each site; the shaded bars represent $\pm 2\sigma$ uncertainty in the measured mean indoor/outdoor nitric acid ratio; the open circles represent model predictions of the indoor/outdoor ratio given the building characteristics shown in Table VI.

Table VI. Input Data for Model Predictions of Indoor/Outdoor HNO_3 Concentration Ratio (C_i/C_o)

site	season	$\bar{f}_{oi}$, m^3/h	f_{ox}, m^3/h	f_{ix}, m^3/h	η_{ox}	η_{ix}	$\sum A_j$, m^2	v_d,[a] m/h
Sepulveda House	summer	2520	0	0	0	0	1710	3.2[b]
	winter	1920	0	0	0	0	1710	3.2
Southwest, main building	summer	15873	0	0	0	0	2081	6.5[c]
	winter	15873	0	0	0	0	2081	6.5
Southwest, California Room	summer	0	267	*d*	0	0	830	2.5
	winter	0	267	*d*	0	0	830	2.5
Norton Simon	summer	0	15080	116000	0.7[e]	0.4[f]	16800	1.4
	winter	0	15080	116000	0.7	0.4	16800	1.4
Scott Gallery, West Wing	summer	0	2530	20700	0[g]	0	3060	6.5
	winter	2530[h]	0	20700	0.5	0.5	3060	6.5
Getty Museum, gallery 121	summer	390	390	4080	0.5	0.5	620	10.0
	winter	360	360	4440	0.5	0.5	620	10.0

[a] Best estimate value for diffusion-limited transport of HNO_3 vapor to the walls of these particular buildings based on the theoretical analysis and experimental data for near-surface air flow (*37*). Same as predicted HNO_3 deposition velocities given in Table IV. [b] Case assumes natural convection-driven flow adjacent to walls when building is closed, and turbulent flow in the core of the room when the building is open to the public. [c] Estimated value assuming turbulent flow in the core of the room. [d] Not determined, as there is no deliberate gaseous pollutant removal applied to the recirculated air. [e] Includes HNO_3 losses from ventilation system filters plus losses in the ductwork. [f] HNO_3 losses in building ductwork and ceiling tiles were treated as a "virtual" filter. [g] An activated carbon filtration system was added between the summer and winter sampling periods. [h] This value was estimated by using the summer PFT air-exchange rate.

conducted at the Scott Gallery before the addition of an activated carbon filter. Revising the modeling analysis of ref 20 to include the activated carbon filter (which removes O_3, thereby suppressing the reaction of O_3 with NO_2) indicates that only 7% of the indoor nitric acid concentration is due to homogeneous chemical production, and therefore, indoor chemical reaction will be neglected in the calculations that follow. The possibility of a change in the equilibrium partitioning between nitric acid and ammonia vapor and aerosol ammonium nitrate due to a change in temperature upon entering a building has been noted (*43*).

If the time-varying parameters in eq 1, such as the air flow rates and the outdoor concentration, are not strongly correlated, then a good approximation to the average ratio of indoor to outdoor concentrations is obtained from the steady-state solution to eq 1:

$$\frac{C_i}{C_o} = \frac{[f_{oi} + (1 - \eta_{ox})f_{ox}]}{[\eta_{ix}f_{ix} + f_{oi} + f_{ox} + \sum_j A_j v_{d_j}]} \qquad (2)$$

In this representation, three groups of factors determine the indoor/outdoor ratio of nitric acid concentrations: (1) the ventilation flow rates, (2) the HNO_3 removal efficiencies by filtration, and (3) the rate of deposition onto surfaces. There are no indoor NO_x sources within these buildings. The Getty museum is attached to an enclosed parking garage, and some possibility for cross-ventilation between the museum and the garage may exist at this site.

The theoretical indoor/outdoor HNO_3 ratio was calculated for each site from eq 2 by using the measured building parameters for each season and the deposition velocity values computed theoretically from data on near-wall air velocities and temperatures. (See Table VI for model input values). In applying the model, it is assumed that the deposition rates predicted for the specific surfaces where fluid motion measurements were made equal the average deposition rates for all interior surfaces. The model results are in reasonable agreement with the experimental data, as shown in Figure 4.

Figure 4 displays the range of indoor to outdoor nitric acid concentration ratios observed at each site during the summer and winter sampling periods. The shaded bars

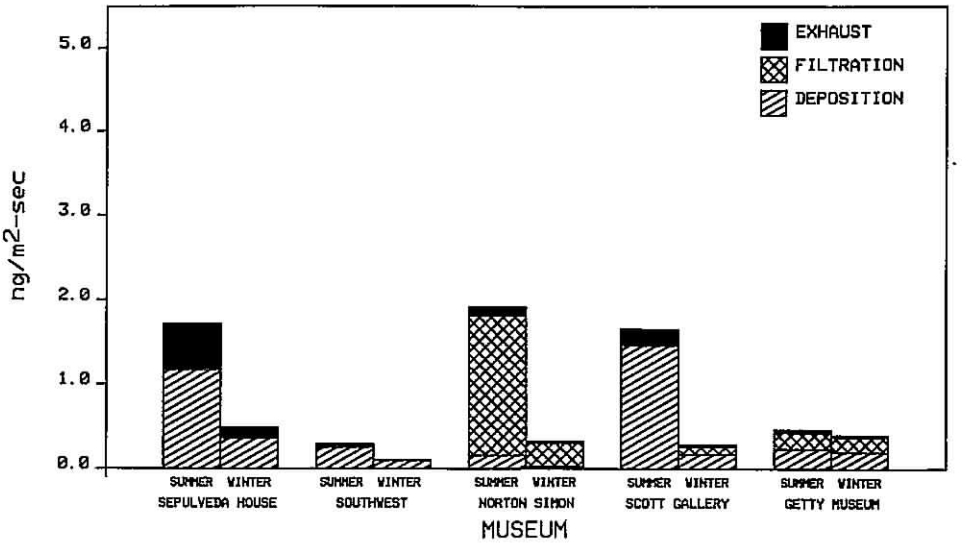

Figure 5. Fate of HNO_3 entering from outdoors. The bars are scaled such that the deposition flux to indoor surfaces can be read in ng/m²·s. Filtration of HNO_3 at the Norton Simon Museum includes the effect of HNO_3 removal during air passage through the ducts and porous ceiling tiles.

represent $\pm 2\sigma$ uncertainty in the measured mean indoor/outdoor nitric acid ratio, while the lower and upper limits of the thin bars on the graph represent the range of indoor/outdoor ratios measured over single 24-h periods during the sampling season. Model predictions of indoor/outdoor nitric acid ratios are depicted by open circles.

In the case of the Southwest Museum, model calculations were performed in two stages. The building parameters for the main galleries at the Southwest Museum were used in eq 2, and a theoretical indoor concentration was obtained. This concentration was then used as the "outdoor" concentration for the California Room since that room draws air from the main portion of the building. At the Norton Simon Museum, the air must travel through a large volume of ductwork in the ventilation system and is then forced through porous ceiling tiles before it enters the galleries. Although activated carbon filtration is not applied in the recirculated air path, measurements show that approximately 40% of the nitric acid is lost to the ducts and ceiling tiles with each recirculated pass. These losses in the ductwork and ceiling at the Norton Simon Museum were treated as a virtual filter with a HNO_3 removal efficiency, η_{ix}, of 40% per pass through the recirculated air path. These ductwork losses were compounded along with the HNO_3 removal efficiency of the ventilation system filters on the inlet air supply to arrive at the initial value of η_{ox}, since that make-up air passes through the ductwork and ceiling before it ever enters the gallery.

At the Scott Gallery, model calculations were conducted without activated carbon filtration during the summer season, but with activated carbon filtration during the winter, corresponding to the actual circumstances. At the Getty Museum, with the open gallery doors, the partitioning of outdoor air supply between infiltration and mechanical ventilation is uncertain, and the flows were estimated to be divided equally between these two sources of outdoor air.

Equation 1 can be used to estimate the fate of HNO_3 entering from outdoors. According to this model, there are three removal routes for HNO_3: (1) deposition to walls and items in the collection, (2) removal by filtration, and (3) expulsion from the building through exfiltration and mechanical exhaust. The fate of HNO_3 at each site is depicted in Figure 5. The values in Figure 5 have been normalized by the interior surface area of each chamber modeled and, thus, represent the flux of HNO_3 (in ng/s·m²) that would deposit on surfaces if it were not removed by another mechanism. At all sites except the Norton Simon Museum, the upper limit on the HNO_3 flux to surfaces indicated by the model (i.e., the size of the bars in Figure 5) is lower than the apparent inorganic nitrate deposition measured from the deposition plates (See Table III). As mentioned previously, it is believed that the deposition plate measurements are influenced by collection of other nitrogenous species in addition to HNO_3, and that the modeled HNO_3 fluxes of Figure 5 provide a reasonable estimate of the actual HNO_3 flux to the indoor surfaces studied.

It is interesting to compare the HNO_3 dose delivered to surfaces at the Norton Simon Museum to the condition at the Scott Gallery during the summer before it was equipped with an activated carbon air filtration system. Both museums are located near Pasadena, CA, and have low indoor HNO_3 concentrations. Both entrain HNO_3 from the outdoor air at an average rate equivalent to approximately 2 ng of HNO_3 per m² of building interior surface area per s. At the Norton Simon Museum, nearly 90% of that HNO_3 burden is removed by collection in the ventilation system. At the Scott Gallery over the summer before the installation of the activated carbon filter, however, the low indoor HNO_3 concentrations were achieved by HNO_3 deposition to indoor surfaces that include the collection. These differences in the indoor deposition rates at the two sites are clearly reflected in the measured apparent deposition rates from the gas phase at the two facilities that are shown in Table III. In short, when low indoor HNO_3 concentrations are observed, it is not a reliable indication that the HNO_3 flux to surfaces will be low. Instead, the low concentrations can be the result of a high flux to the indoor surfaces.

Conclusions

The HNO_3 concentrations in indoor and outdoor air have been measured for summer and winter seasons at five museums in southern California. In summer months, outdoor HNO_3 concentrations average 4.2–7.7 $\mu g/m^3$ (1.6–3 ppb) at the four heavily urbanized sites studied, while outdoor HNO_3 concentrations in winter average 1.2–2.2 $\mu g/m^3$ (0.5–0.9 ppb). At one museum where a high rate of infiltration of air through open doors and windows provides the sole means of ventilation, indoor HNO_3 levels average from 36% (summer) to 40% (winter) of those outdoors, with some 24-h periods showing indoor HNO_3 levels 69% as high as those outdoors. In contrast, indoor

HNO_3 concentrations generally below 0.1 $\mu g/m^3$ (0.04 ppb) (about 1% of that outdoors) are measured inside a second museum that features a very low flow rate of outdoor make-up air, a high internal air recirculation rate, and activated carbon filtration of the make-up air supply. The single-pass HNO_3 removal efficiency of the activated carbon plus particle filters present in the latter museum's ventilation system was measured to be 49%. This shows that the low indoor HNO_3 concentrations at that site are only partly due to deliberate pollutant removal; loss of HNO_3 to surfaces within the ventilation system, ceiling tiles, and indoor building surfaces also must occur in order for the indoor HNO_3 concentration to approach 1% of that outdoors.

Deposition plates for the collection of inorganic nitrate were attached to the interior walls of the museums studied. A total inorganic nitrate accumulation on nylon surfaces as high as 5.85 $ng/m^2 \cdot s$ during the summer season is observed at the site with the highest indoor pollutant levels, falling to 0.18 $ng/m^2 \cdot s$ at the site with the most effective pollution control system. Deposition velocities computed from the deposition data and indoor HNO_3 concentrations suggest that the inorganic nitrate accumulation is too high to be due to HNO_3 alone; the fluxes exceed the HNO_3 entering the building from outdoors in four of the five cases if the accumulation was due solely to HNO_3 dry deposition. Other gas-phase nitrogeneous species are believed to be contributing to the inorganic nitrate accumulation observed.

An indoor/outdoor air quality model was used to compute the indoor HNO_3 concentrations expected given the outdoor HNO_3 concentrations and data on building ventilation system design. Model predictions of the indoor/outdoor HNO_3 concentration ratio overlap the range of measured indoor/outdoor HNO_3 concentration ratios in 8 of the 10 cases modeled. The modeling calculations show that HNO_3 deposition on interior surfaces is often the principal sink for HNO_3, which accounts for the low HNO_3 concentrations observed indoors. This suggests that one should interpret low indoor HNO_3 concentration measurements very carefully when assessing the potential for damage to museum collections: the low indoor HNO_3 concentrations may be the result of a high pollutant flux to indoor surfaces that include the collections.

Acknowledgments

We thank Theresa Fall and Paul Solomon for assistance in maintaining the air monitoring network. We also thank the staff at the following museums for their help in providing access to the museum sampling sites: the Sepulveda House, the Southwest Museum, the Norton Simon Museum, the Virginia Steele Scott Gallery, and the J. Paul Getty Museum.

Registry No. HNO_3, 7697-37-2.

Literature Cited

(1) Baer, N. S.; Banks, P. N. *Int. J. Mus. Manage. Curator.* **1985**, *4*, 9–20.
(2) *Air quality criteria for oxides of nitrogen*; EPA 600/8-82-026; U.S. Environmental Protection Agency: Research Triangle Park, NC 1982.
(3) Giles, C. H. *J. Appl. Chem.* **1965**, *15*, 541–550.
(4) Ajax, R. W.; Conlee, C. J.; Upham, J. B. *J. Air Pollut. Control Assoc.* **1967**, *17*, 220–224.
(5) Beloin, N. J. *Text. Chem. Color.* **1972**, *4*, 43–48.
(6) Bryson, R. J.; Trask, B. J.; Upham, J. B.; Booras, S. G. *J. Air Pollut. Control Assoc.* **1967**, *17*, 294–298.
(7) Zeronian, S. H.; Alger, K. W.; Omaye, S. T. *Proceedings of the Second International Clean Air Congress*, Washington, DC, December 1970; Academic Press, Inc.: New York, 1971; pp 468–476.
(8) Hermance, H. W.; Russell, C. A.; Bauer, E. J.; Egan, T. F.; Wadlow, H. V. *Environ. Sci. Technol.* **1971**, *5*, 781–785.
(9) Johansson, L. G. *J. Electrochem. Soc.* **1985**, *132*, 221.
(10) Edney, E. O.; Stiles, D. C.; Haynie, F. H.; Spence, J. W.; Wilson, W. E. *ACS Symp. Ser.* **1986**, *No. 318*, 172–193.
(11) Zakipour, S.; Leygraf, C. *J. Electrochem. Soc.* **1986**, *133*, 21–30.
(12) Sinclair, J. D.; Weschler, C. J. *ACS Symp. Ser.* **1986**, *No. 318*, 216–223.
(13) Graedel, T. E.; McGill, R. *Environ. Sci. Technol.* **1986**, *22*, 1093–1100.
(14) Whitmore, P. M.; Cass, G. R. *Stud. Conserv.* **1989**, *34*, 85–97.
(15) Eastlake, C. L.; Faraday, M.; Russell, W. Report on the protection by glass of the pictures in the National Gallery, House of Commons, 24 May 1850.
(16) Thomson, G. *Stud. Conserv.* **1965**, *10*, 147–168.
(17) Shaver, C. L.; Cass, G. R.; Druzik, J. R. *Environ. Sci. Technol.* **1981**, *17*, 748–752.
(18) Davies, T. D.; Ramer, B.; Kaspyzok, G.; Delany, A. C. *J. Air Pollut. Control Assoc.* **1984**, *31*, 135–137.
(19) Druzik, J. R.; Adams, M. S.; Tiller, C.; Cass, G. R. *Atmos. Environ.*, in press.
(20) Nazaroff, W. W.; Cass, G. R. *Environ. Sci. Technol.* **1986**, *20*, 924–934.
(21) Hackney, S. *Stud. Conserv.* **1984**, *29*, 105–116.
(22) Spicer, C. W.; Howes, J. E.; Bishop, T. A.; Arnold, L. H.; Stevens, R. K. *Atmos. Environ.* **1982**, *16*, 1487–1500.
(23) Grosjean, D. *Environ. Sci. Technol.* **1983**, *17*, 13–19.
(24) Solomon, P. A.; Fall, T.; Salmon, L. G.; Lin, P.; Vasquez, F.; Cass, G. R. Acquisition of acid vapor and aerosol concentration data for use in dry deposition studies in the South Coast Air Basin. EQL Report 25; Environmental Quality Laboratory, California Institute of Technology, Pasadena, CA. Final report submitted to the California Air Resources Board, March, 1988.
(25) Solomon, P. A.; Larson, S. M.; Fall, T.; Cass, G. R. *Atmos. Environ.* **1988**, *22*, 1587–1594.
(26) Hering, S. V.; Lawson, D. R.; et al. *Atmos. Environ.* **1988**, *22*, 1519–1539.
(27) Russell, A. G.; Cass, G. R. *Atmos. Environ.* **1984**, *18*, 1815–1827.
(28) Shaw, R. W.; Stevens, R. K.; Bowermaster, J.; Tesch, J. W.; Tew, E. *Atmos. Environ.* **1982**, *16*, 845–853.
(29) Forrest, J.; Spandau, D. J.; Tanner, R. L.; Newman, L. *Atmos. Environ.* **1982**, *16*, 1473–1485.
(30) John, W.; Reischl, G. *J. Air Pollut. Control Assoc.* **1980**, *30*, 872–876.
(31) Ligocki, M. P.; Salmon, L. G.; Fall, T.; Jones, M. C.; Cass, G. R. Submitted for publication in *Atmos. Environ.*
(32) Appel, B. R.; Tokiwa, Y.; Haik, M. *Atmos. Environ.* **1981**, *15*, 283–289.
(33) Pierson, W. R.; Brachaczek, W. W.; Japar, S. M.; Cass, G. R.; Solomon, P. A. *Atmos. Environ.* **1988**, *22*, 1657–1663.
(34) Dietz, R. N.; Cote, E. A. *Environ. Int.* **1982**, *8*, 419–433.
(35) Dietz, R. N.; Goodrich, R. W.; Cote, E. A.; Wieser, R. F. *Measured Air Leakage of Buildings, ASTM STP 904*; Trechsel, H. R., Lagus, P. L., Eds., ASTM: Philadelphia, PA, 1986; pp 203–264.
(36) ASHRAE *ASHRAE Handbook: 1985 Fundamentals*; American Society of Heating, Refrigeration and Air-Conditioning Engineers: Atlanta, GA 1985; Chapter 22.
(37) Nazaroff, W. W. Mathematical modeling and control of pollutant dynamics in indoor air. Ph.D. Thesis, California Institute of Technology, Pasadena, 1989.
(38) Nazaroff, W. W.; Ligocki, M. P.; Ma, T.; Cass, G. R. *Aerosol Sci. Technol.*, in press.
(39) Perrino, C.; DeSantis, F.; Febo, A. *Atmos. Environ.* **1988**, *22*, 1925–1930.
(40) Yamanaka, S. *Environ. Sci. Technol.* **1984**, *18*, 566–570.
(41) Pitts, J. N., Jr.; Wallington, T. J.; Biermann, H. W.; Winer, A. M. *Atmos. Environ.* **1985**, *19*, 763–767.
(42) Shair, F. H.; Heitner, K. L. *Environ. Sci. Technol.* **1974**, *8*, 444–451.

(43) Nazaroff, W. W.; Cass, G. R. *Environ. Sci. Technol.* **1989**, *23*, 157–166.

Received for review November 14, 1989. Accepted March 12, 1990. This publication is based upon research that was supported (in part) by a Research Agreement from the Getty Conservation Institute. Any opinions, findings, and conclusions or recommendations expressed in this publication are those of the author(s) and do not necessarily reflect the views of the Getty Conservation Institute of the J. Paul Getty Trust.